

# On the Cable Actuation of End-Effector Degrees of Freedom in Cable-Driven Parallel Robots

Jean-Baptiste Izard<sup>1</sup> and Marc Gouttefarde<sup>2</sup>

<sup>1</sup> Alted, Clapiers, France

<sup>2</sup> LIRMM, Univ Montpellier, CNRS, Montpellier, France  
jbi@alted.fr

**Abstract.** By routing the cables that support and drive the mobile platform of a Cable-Driven Parallel Robot (CDPR) to the moving parts of an end-effector (EE) installed on said mobile platform, it is possible with combined motions of the winches of the CDPR to drive this EE, such as the opening and closing of a gripper. Compared to CDPRs without internal EE, the cable tension distribution is then modified. In this paper, the static equilibrium of a CDPR platform with an internal EE driven by the supporting cables is analyzed, showing that an additional platform wrench needs to be balanced when force is applied on the EE. Both the magnitude of the wrench on the EE degrees of freedom and the way the cables generate motion at the EE influence this additional platform wrench. Considering a cable configuration and an external wrench applied on the EE, several EE designs are proposed where the EE motion is driven by one or two cables leading to different results in terms of workspace and wrench feasibility.

**Keywords:** Platform internal end-effector motion, static equilibrium, wrench-feasible workspace analysis, available wrench set analysis.

## 1 Introduction

Cable-Driven Parallel Robots (CDPRs) and Delta-type parallel robots share one design issue in industrial applications: Creating additional large-amplitude Degrees Of Freedom (DOFs) at the mobile platform leads in both cases to significant complexity. In the case of the Delta robot, the dynamic capabilities rely partly on having a lightweight mobile platform, but integrating an actuator in the platform adds weight. In addition, electric and pneumatic cables can be damaged by the numerous bending cycles and flutters caused by the rapid movements of the platform. In the case of CDPRs, most applications require motion at the end-effector (EE) mounted on the mobile platform: at least one DOF is generally required, frequently two, for instance generating a large rotation together with opening and closing a gripper. Space into the mobile platform and payload capabilities may not be an issue. However, when the workspace dimensions are large, it is complex to realize an electrical and/or pneumatic harness, connecting the platform to the robot base structure, which is reliable, cost-effective and does not hinder the platform movements.

In Delta robots, the problem has been circumvented by using one or more UPU kinematic chains in parallel to the three Delta kinematic chains. A notable design, proposed for the PAR4 and used in the Quattro robot marketed by Omron [1], consists in adding a fourth R-PAR actuated kinematic chain, identical to the original 3 Delta chains, and using the resulting actuation redundancy to generate a rotation created by means of an articulated mobile platform. This design has limited impact on the dynamics and workspace size of the robot. Other similar concepts have since emerged to add a DOF to the platform of a Delta-like robot, e.g. [2, 3], but none of them provides more than one DOF and all of them are based on rigid-link kinematic chains.

Rotational limitations in CDPRs have also led to design specific configurations that are able to generate a large rotation within the mobile platform. In [4], a rotational DOF within the platform is directly actuated by cables to generate rotations of large amplitudes. Another new type of spatial CDPR providing unlimited rotations about an axis is presented in [5]. In this particular design, eight cables are wrapped around a cylindrical mobile platform. In [6], a planar CDPR with infinite platform rotation is introduced. It uses a mechanism embedded into the mobile platform actuated from the CDPR base by a cable loop and does not suffer from parasitic motions. Moreover, full unlimited 3-DOF rotations are obtained in [7, 8] by using an embedded spherical wrist implemented with omni-wheels.

On the other hand, 6-DOF CDPRs are often redundantly actuated, typically using eight cables, in order to achieve large workspaces and/or to fully constrain the mobile platform. This actuation redundancy may also be used to drive additional motions inside the mobile platform. There are many ways to route cables inside a CDPR platform using pulleys and eyelets which direct them towards mobile elements to which they are attached [9]. This creates internal mobility within the platform, driven by the cables, but this also has an impact on the cable tensions. It is crucial for the operation of the CDPR that the introduction of this internal mobility does not hinder the static equilibrium of the platform.

The first contribution of this paper is the mathematical analysis of a CDPR with  $n > 6$  degrees of freedom and  $m \geq n$  cables in order to determine the impact of introducing internal EE motions to an existing CDPR design, in particular in how it impacts the wrench applied to the platform.

Several ways to drive internal EE DOFs constructed on the base of an 8-cable suspended CDPR configuration are then proposed and analyzed to compare their performance in terms of wrench capabilities and workspace. This analysis considers one internal EE DOF but could be generalized to more DOFs in future works. From this perspective of wrench modification, designs suggested in [4, 7, 8] are discussed.

## 2 Wrench equations

Singularities set aside, a set of  $n$  actuators can fully drive up to  $n$  DOFs. A CDPR is redundantly actuated when there are more actuators than mobile platform DOFs: at a given platform pose, there exists infinitely many cable tension combinations that can balance a given wrench at the mobile platform. The same mechanism with less actuators

than mobile platform DOFs is underactuated: at a given pose, only a limited set of wrenches can be balanced by cable tensions. Isostatic mechanisms have as many actuators as DOFs, and one combination of cable tensions corresponds to one platform wrench (and vice-versa).

The vector of cable forces  $\boldsymbol{\tau}$  is mapped into the wrench  $\boldsymbol{f}$  through the wrench matrix  $\boldsymbol{W}$  with  $n$  rows and  $m$  columns. The CDPR is fully actuated at the necessary condition that the rank of  $\boldsymbol{W}$  is equal to  $n$ . With forces and velocities being dually linked,  $\boldsymbol{W}$  can also be used to calculate the vector  $\dot{\boldsymbol{l}}$  of cable length time derivatives (cable velocities) in function of the platform twist  $\boldsymbol{t}$ .

$$\boldsymbol{f} = \boldsymbol{W}\boldsymbol{\tau} \quad ; \quad \dot{\boldsymbol{l}} = -\boldsymbol{W}^T\boldsymbol{t} \quad (1)$$

The column vector  $\boldsymbol{w}_i$  of  $\boldsymbol{W}$ , of dimension  $n$ , represents the wrench generated by cable  $i = 1..m$  at the level of the mobile platform for a unit cable force. In the case of a CDPR with massless cables, vectors  $\boldsymbol{w}_i$  have a well-known expression given in Eq. (2), with  $\boldsymbol{b}_i$  the vector representing the position vector of cable  $i$  attachment point to the mobile platform in the platform reference frame, and  $\boldsymbol{u}_i$  the unitary vector directed along the cable segment from the platform to the base.

$$\boldsymbol{W} = [\boldsymbol{w}_1 \quad \boldsymbol{w}_2 \quad \cdots \quad \boldsymbol{w}_m] \quad ; \quad \boldsymbol{w}_i = \begin{pmatrix} \boldsymbol{u}_i \\ \boldsymbol{b}_i \times \boldsymbol{u}_i \end{pmatrix} \quad (2)$$

Another description of  $\boldsymbol{W}$  is given in Eq. (3) where the row vectors  $\boldsymbol{v}_j, j = 1..n$ , correspond to the rows of  $\boldsymbol{W}$ ;

$$\boldsymbol{W} = [\boldsymbol{v}_1^T \quad \boldsymbol{v}_2^T \quad \cdots \quad \boldsymbol{v}_n^T]^T \quad (3)$$

Each  $\boldsymbol{v}_j$  corresponds to the cable velocities that generate a movement on one of the translational or rotational degrees of freedom  $j$  of the mobile platform.

Let us consider a CDPR with  $m$  cables to which we add a supplementary cable  $m + 1$ . The cable tension vector  $\boldsymbol{\tau}$  therefore gains an element, the cable tension  $\tau_{m+1}$ . Moreover, the wrench matrix  $\boldsymbol{W}$  gains a column  $\boldsymbol{w}_{m+1}$  representing the wrench generated by cable  $m + 1$  for a unit cable force. All platform DOFs being potentially impacted by this new cable, all components of  $\boldsymbol{w}_{m+1}$  are likely to be non-zero.

On the other hand, adding an internal EE motion in the mobile platform leads to adding an element to the wrench  $\boldsymbol{f}$ , corresponding to the force or moment  $f_{n+1}$  to be generated on the EE DOF, and adding a row  $\boldsymbol{v}_{m+1}$  to  $\boldsymbol{W}$  built from the combination of cable velocities that generate a movement along this new DOF.

Let us now consider a CDPR with  $m$  cables,  $n$  degrees of freedom and  $k \leq m - n$  internal EE DOFs driven by the cables. The wrench  $\boldsymbol{f}$  is then composed of the wrench  $\boldsymbol{f}_n$  applied on the platform and of a set of forces/moments  $\boldsymbol{f}_k, k = 1 \dots m - n$  on the platform internal EE DOFs. The wrench matrix  $\boldsymbol{W}$  can be decomposed in two submatrices:  $\boldsymbol{W}_{n \times m}$ , the wrench matrix of the CDPR if there were no internal EE motion, as described in Eq. (2), and  $\boldsymbol{W}_{k \times m}$ , the wrench matrix of the EE DOFs considered individually. These two matrices are considered to have full rank. Eq. (1) then becomes:

$$\begin{bmatrix} \mathbf{f}_n \\ \mathbf{f}_k \end{bmatrix} = \begin{bmatrix} \mathbf{W}_{n \times m} \\ \mathbf{W}_{k \times m} \end{bmatrix} \boldsymbol{\tau} \quad (4)$$

### 3 Evaluation of static equilibrium

This section presents an analysis of the Constant-Orientation Wrench-Feasible Workspace (COWFW) and Available Wrench Set (COAWS) of various designs of CDPRs having internal EE DOFs. An example CDPR configuration is crafted taking inspiration from the CoGiRo CDPR configuration [10]. It sits on a footprint measuring 12 x 8 x 6 m, with a box-shaped mobile platform frame measuring 1 x 1.4 x 1.5 m. The platform reference point is at the center of the pattern drawn by the cable fixing points on the lower side of the platform. The empty platform weighs  $m_0=150$  kg. The coordinates of the center of mass of the empty platform are (0,0,0.75) m. The resulting 6D wrench from gravity is denoted  $\mathbf{f}_6$ . The cable diameter is 4 mm, weighing 65 g per meter. Winches are designed with a safe working load of 2500 N (security factor of 4).

**Table 1.** Example configuration drawing and fixing point coordinates in m.

Cable #	1	2	3	4	5	6	7	8	
Drawing points	X	-5.5	-6	6	5.5	5.5	6	-6	-5.5
	Y	-4	-3.5	-3.5	-4	4	3.5	3.5	4
	Z	6	6	6	6	6	6	6	6
Fixing points	X	0.5	-0.5	0.6	-0.5	-0.5	0.5	-0.6	0.5
	Y	-0.8	0.7	0.7	-0.7	0.8	-0.7	-0.7	0.7
	Z	0	1.5	0	1.5	0	1.5	0	1.5

The purpose of the CDPR is to carry a payload  $f_{EE}=500$  N that comes in addition to the platform weight. A vertical translational EE DOF is considered: the purpose of the EE is to move the payload up and down. We consider that  $f_{EE}$  is applied vertically right below the platform reference point, therefore an additional platform wrench  $\mathbf{f}_{EE} = (0,0,f_{EE},0,0,0)^T$  adds up to  $\mathbf{f}_6$  when the load is carried.

Different designs derived from this configuration will be evaluated in terms of COWFW and COAWS in sections 3.3 to 3.6. Details on how the COWFW and COAWS are calculated are given in sections 3.1 and 3.2, respectively.

#### 3.1 Wrench-feasible workspace analysis

The COWFW is the set of positions of the CDPR mobile platform where a given external wrench or set of wrenches can be balanced by a set of cable tensions within a feasible tension set. The latter is defined as non-negative lower and upper bounds on the cable tensions. The lower bounds are defined for each cable as the positive cable tension required to have a length to sag ratio of 5 [11]. The upper bound is defined by the safe

working load of the winch. The method detailed in [10] is used to test if a given pose belongs to the COWFW. Validity of a pose is also conditioned to cables not colliding with the platform. With the CoGiRo CDPR cable configuration, no collision occurs between the cables for any pose at reference orientation within the footprint.

The search of the COWFW boundary is performed by testing a set of directions covering the space around the reference pose which is to be tested valid beforehand. Each direction is tested with a bisection algorithm and outputs a boundary position. All boundary positions are arranged to shape a boundary surface.

### 3.2 Available wrench set analysis

The COAWS can be defined as the set of wrenches that can be balanced by a cable tension set, with values within a feasible tension set, for all platform positions within a prescribed set, the platform orientation being fixed at the reference orientation. The tension feasible set is defined as in section 3.1. At each position, the COAWS is calculated using the hyperplane shifting method detailed in [12]. The COAWS for the given set of positions is the intersection of the COAWS of all individual positions. In the following analysis, the prescribed set of positions is a meshing of the constant orientation workspace representing  $2/3$  of the horizontal footprint dimensions and  $1/2$  of the vertical footprint dimension. This workspace corresponds to the prescribed one in the optimization of the CoGiRo CDPR configuration [10], with the exclusion of rotations.

Once the COAWS is built, the intersection of the COAWS with a subspace of the wrench space, where some wrench components are fixed, can be computed. In the following, all platform wrench components are set at 0 except for the vertical force.

The wrench coordinate  $f_z$  along the vertical force direction is thereafter transformed into admissible additional mass to the platform  $m_{add}$  through the following equation:

$$m_{add} = -\frac{f_z}{g_0} - m_0 \quad (5)$$

where  $g_0$  is the acceleration of gravity equal to  $9.81 \text{ m/s}^2$ , and  $m_{add}$  indicates the additional weight that the platform can be carry on top of platform empty weight.

In cases where the EE is driven by a combination of cables, another variable in the wrench is the force applied on the EE embedded in the platform. In the 2D space with coordinates in  $m_{add}$  and  $f_{EE}$ , the COAWS is a convex polygon. Moreover, we consider that the force  $f_{EE}$  drives the added mass  $m_{add}$  with a speed reduction ratio of  $1/\eta$ . A given value of  $m_{add}$  carried by  $f_{EE}$  requires  $\eta$  to be equal to  $m_{add}g_0/f_{EE}$ .

### 3.3 EE DOF driven independently

In a first design, the EE is driven independently from the cables. This is the reference design to which the designs discussed in the next sections will be compared. The effects of physically installing the EE actuators on board of the platform (transmission of energy and signal to the platform) are ignored.

Fig. 1 shows the corresponding COWFW, which size is evaluated at 9.6 x 6.3 x 4.0 m. As for the COAWS, the only variable left is  $m_{add}$ , valid from 0 to 261 kg.

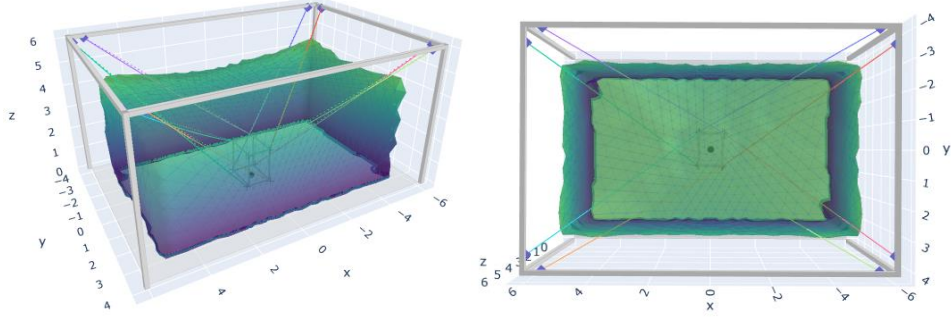


**Fig. 1.** COWFW of the example configuration with a translational EE DOF driven separately against  $f_{EE} = 500$  N. Coordinates are shown in m.

### 3.4 Directly wiring a cable to the EE DOF

A direct solution to drive an internal EE DOF with a cable of a CDPR would be to draw one cable on the platform through an eyelet and then route this cable into the platform to actuate the internal EE DOF.

Let us consider the example configuration defined at the beginning of Section 3. Instead of being fixed to the platform, cable 1 is run on an eyelet and routed to the payload through a block and pulley mechanism with  $\eta$  cable leads routed on the block. This corresponds to a reduction ratio of  $1/\eta$ . With  $\mathbf{w}_1 \dots \mathbf{w}_8$  the columns of the wrench matrix of the configuration at the considered position without the driving of the EE DOF, Eq. (4) writes:

$$\begin{bmatrix} \mathbf{f}_6 + \mathbf{f}_{EE} \\ f_{EE} \end{bmatrix} = \begin{bmatrix} \mathbf{w}_1 & \mathbf{w}_2 \dots \mathbf{w}_8 \\ \eta & \mathbf{0}_{1 \times 7} \end{bmatrix} \boldsymbol{\tau} \quad ; \quad \mathbf{w}_i = \begin{pmatrix} \mathbf{u}_i \\ \mathbf{b}_i \times \mathbf{u}_i \end{pmatrix}, \quad i = 1 \dots 8 \quad (6)$$

This solves into the following equation:

$$\tau_1 = \frac{f_{EE}}{\eta} \quad ; \quad \mathbf{f}_6 + \mathbf{f}_{EE} - \mathbf{w}_1 f_{EE} / \eta = [\mathbf{w}_2 \dots \mathbf{w}_8] \boldsymbol{\tau}_{2..8} \quad (7)$$

This equation corresponds to setting  $\tau_1$  equal to  $f_{EE}/\eta$  and thereafter solving the static equilibrium of the CDPR using only cables 2 to 8, with the gravity wrench  $\mathbf{f}_6$  being incremented by  $-\mathbf{w}_1 f_{EE}/\eta$ , which is the effect of the cable 1 with tension  $\tau_1$ .

Considering all positions in the prescribed set leads to an empty COAWS, i.e. it is not possible to carry a payload of any magnitude this way in all positions. Four subsets of positions are then determined, which lead to different COAWS that do not intersect (Fig. 3).

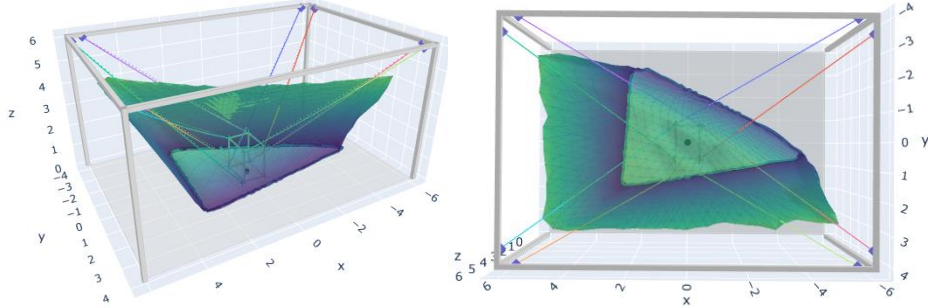


**Fig. 2.** COWFW of the example configuration where the translational EE is driven by cable 1 (blue cable) against  $f_{EE} = 500$  N with  $\eta = 1$ . Coordinates are shown in m.

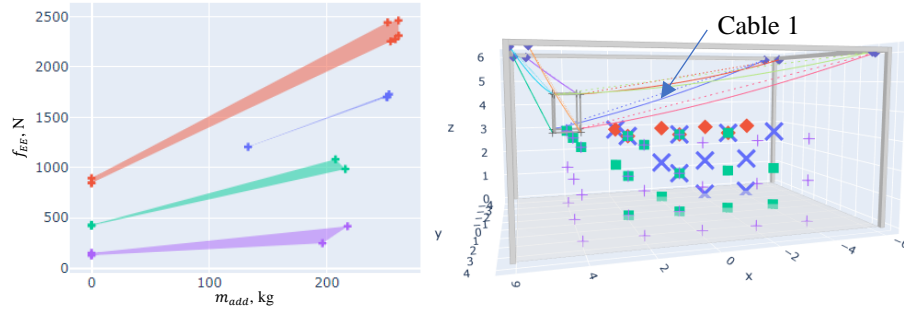


**Fig. 3.** AWS of the design featuring cable 1 driving the translational EE DOF. The AWS is shown on the left, and corresponding position sets are shown with the same colors on the right, where coordinates are shown in m.

### 3.5 Doubling a cable to drive a drum

The designs proposed in [7, 9] are meant to modify a CDPR cable configuration by selecting a cable which is doubled. Both cables from this doubling are driven by individual winches. Inside the platform, these cables are routed to a drum where they are wound in opposite directions. Running the winches of these two cables in opposite directions therefore actuate the internal EE DOF.

Let us select cable 1 of a configuration and double it. The two corresponding cables are numbered 0 and 1, increasing the total number of cables to  $m + 1$ . The fixing and drawing points of cables 0 and 1 are built from the former positions of the fixing and drawing point of cable 1: both are moved by a position vector denoted  $\mathbf{d}_{01}$  in opposite directions in order to keep the unit vectors  $\mathbf{u}_0$  and  $\mathbf{u}_1$  directing cables 0 and 1 equal.

$$\begin{bmatrix} \mathbf{f}_6 + \mathbf{f}_{EE} \\ f_{EE} \end{bmatrix} = \begin{bmatrix} (\mathbf{b}_1 + \mathbf{d}_{01}) \times \mathbf{u}_1 & (\mathbf{b}_1 - \mathbf{d}_{01}) \times \mathbf{u}_1 & \mathbf{w}_2 \cdot \mathbf{w}_m \\ \eta & -\eta & \mathbf{0}_{1 \times m-1} \end{bmatrix} \boldsymbol{\tau} \quad (8)$$

Eq. (8) shows the wrench matrix for this configuration. Changing coordinates for  $\boldsymbol{\tau}$ , replacing  $\tau_0$  and  $\tau_1$  by  $\tau_1^+ = \tau_0 + \tau_1$  and  $\tau_1^- = \tau_0 - \tau_1$  respectively, leads to:

$$\begin{bmatrix} \mathbf{f}_6 + \mathbf{f}_{EE} \\ f_{EE} \end{bmatrix} = \begin{bmatrix} \mathbf{0}_3 & \mathbf{w}_1 & \mathbf{w}_2 \cdot \mathbf{w}_m \\ (\mathbf{d}_{01} \times \mathbf{u}_1) & 0 & \mathbf{0}_{1 \times m-1} \\ 2\eta & & \end{bmatrix} [\tau_1^- \quad \tau_1^+ \quad \tau_2 \dots \tau_m]^T \quad (9)$$

Which solves into the following set of equations:

$$\tau_1^- = f_{EE}/2\eta ; \quad \mathbf{f}_6 + \mathbf{f}_{EE} - \underbrace{\left( \mathbf{d}_{01} \times \mathbf{u}_1 \right) f_{EE}/2\eta}_{\mathbf{f}_6^+} = [\mathbf{w}_1 \cdot \mathbf{w}_m] [\tau_1^+ \quad \tau_{2..m}]^T \quad (10)$$

This set of equations corresponds to the static equilibrium of the CDPR without the internal EE, where the tension in former cable 1 is replaced by the sum  $\tau_1^+$  of the tensions in cables 0 and 1, and to which an extra wrench noted  $\mathbf{f}_6^+$ , with only torque values, adds to gravity wrench  $\mathbf{f}_6 + \mathbf{f}_{EE}$ . The magnitude of  $\mathbf{f}_6^+$  is proportional to  $f_{EE}$  and to the norm of the cross product  $\mathbf{d}_{01} \times \mathbf{u}_1$ .

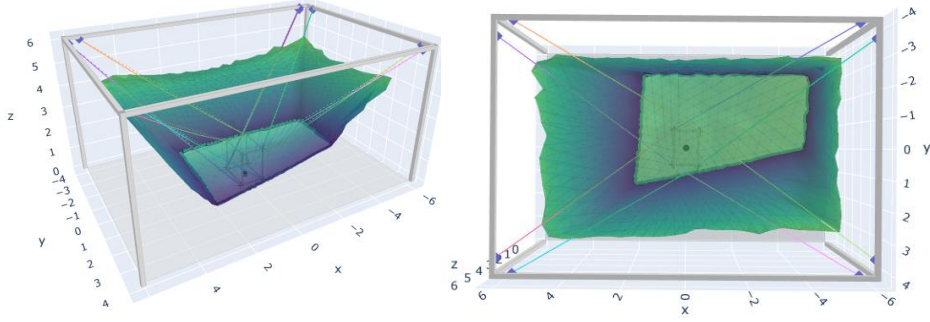


**Fig. 4.** COWFW with the translational EE driven by a combination of cable 0 and cable 1 obtained by doubling original cable 1 against  $f_{EE} = 500$  N with  $\eta = 1$ . Coordinates are in m.

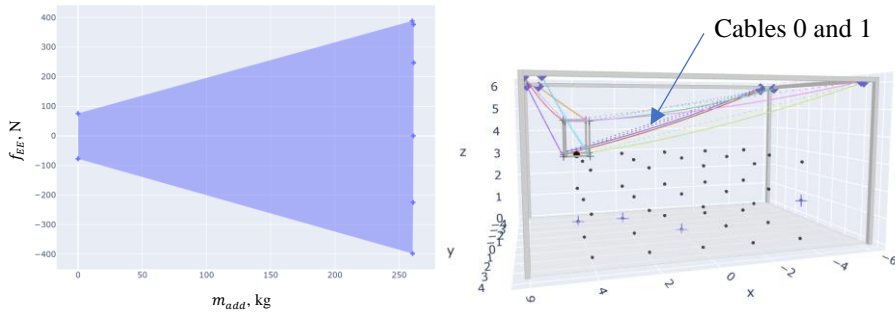


**Fig. 5.** COAWS of the example configuration with cable 1 being doubled to drive a translational EE DOF. Limiting positions are shown on the right as blue crosses. Black dots show non-limiting feasible positions which are part of the prescribed set of positions.



In order to evaluate this design, the example configuration is modified by doubling cable 1 with  $d_{01} = [0 \ 0 \ 0.1m]^T$ .  $f_{EE}$  is once again set equal to 500 N and  $\eta$  to 1. The COWFW and COAWS are shown in Fig. 4 and Fig. 5.

In the case of the robot presented in [7, 8] with 6 degrees of freedom and 8 cables, cables are assembled by pairs which are routed towards 4 actuated drums installed in the platform. Middle points of fixing point pairs shape a square.  $f_{EE}$  is replaced by a vector of torques  $(f_{EE_i})^T, i = 1..4$ , actuated on the drums, with  $\eta$  matching the radius of the drums. Cable tensions are denoted  $\tau_{ij}, i = 1..4$  and  $j = 1..2$ ,  $\tau_i^+ = \tau_{i1} + \tau_{i2}$  and  $\tau_i^- = \tau_{i1} - \tau_{i2}$ , Eq. (4) becomes the following equation:

$$\begin{bmatrix} \mathbf{f}_6 + \mathbf{f}_{EE} \\ (f_{EE_1} \dots f_{EE_4})^T \end{bmatrix} = \sum_{i=1..4} \begin{bmatrix} \mathbf{0}_3 & \mathbf{w}_i \\ \mathbf{d}_i \times \mathbf{u}_i & 2\eta \\ \mathbf{0}_{1 \times m-1} & \end{bmatrix} \begin{bmatrix} \tau_i^+ \\ \tau_i^- \end{bmatrix} \quad (11)$$

which solves into Eq. (12), corresponding to an underactuated CDPR with 4 cables attached to the platform at the vertices of a square, with the addition of a perturbation wrench  $\mathbf{f}_6^+$  with non-zero values on torque directions proportional to values  $f_{EE_i}$ , which is applied in addition to  $\mathbf{f}_6$ :

$$\begin{cases} \tau_{i1} - \tau_{i2} = 2f_{EE_i}/\eta, \quad i = 1..4 \\ \mathbf{f}_6 + \mathbf{f}_{EE} - \underbrace{\sum_{i=1..4} 2 \begin{pmatrix} \mathbf{0}_3 \\ \mathbf{d}_i \times \mathbf{u}_i \end{pmatrix} f_{EE_i}/\eta}_{\mathbf{f}_6^+} = [\mathbf{w}_1 \dots \mathbf{w}_4] [\tau_i^+]_{i=1..4} \end{cases} \quad (12)$$

With the CDPR being underactuated, this perturbing wrench leads to a perturbation of the position. This would explain why, in [8], the platform shows erratic movements when EE motion is performed while the platform is suspended. Friction in the drums require torque from the EE DOFs, which turn into additional wrench on the platform. As the CDPR static equilibrium is equivalent to that an underactuated cable configuration, this wrench generates the shift in position and orientation visible in the video in [8].

### 3.6 Running a pair of cables towards a drum carrying the load

The design proposed in [4] features a platform built with a vertical central rod to which 6 cables are attached in 2 clusters of 3 cables drawn upwards and downwards, which makes for an overconstrained CDPR with 5 DOF, excluding the rotation of the central rod. The central rod is then fixed by a drum coaxial to it to which two cables are attached, drawn from the base in a mostly horizontal direction, in order to pull on the drum in antagonistic directions. Similar constructions are also proposed in [9].

We therefore study in this section the design where two cables from the initial configuration are taken through an eyelet to an EE with a reduction ratio  $1/\eta$ . The number of cables is unchanged. The wrench matrix is augmented with a row vector with non-zero values for the cables driving the EE and 0 for the other cables. We choose to drive the EE with cables 1 and 2. With  $\tau_{12}^+ = \tau_1 + \tau_2$  and  $\tau_{12}^- = \tau_1 - \tau_2$ , Eq. (4) leads to:

$$\begin{bmatrix} \mathbf{f}_6 + \mathbf{f}_{EE} \\ f_{EE} \end{bmatrix} = \begin{bmatrix} \mathbf{w}_1 - \mathbf{w}_2 & \mathbf{w}_1 + \mathbf{w}_2 & \mathbf{w}_3 \dots \mathbf{w}_m \\ 2\eta & 0 & \mathbf{0}_{1 \times m-2} \end{bmatrix} [\tau_{12}^- \quad \tau_{12}^+ \quad \tau_3 \dots \tau_m]^T \quad (13)$$

which solves into Eq. (14), which corresponds to the static equilibrium of a modification of the original configuration where a cable runs from drawing point 1 to fixing point 1, then through eyelets and pulleys to fixing point 2, and then to drawing point 2; and to which an additional wrench  $\mathbf{f}_6^+$  is applied, proportional to  $f_{EE}$ :

$$\begin{cases} \tau_{12}^- = \frac{f_{EE}}{2\eta} \\ \mathbf{f}_6 + \mathbf{f}_{EE} - \underbrace{(\mathbf{w}_1 - \mathbf{w}_2) \frac{f_{EE}}{2\eta}}_{\mathbf{f}_6^+} = [(\mathbf{w}_1 + \mathbf{w}_2) \quad \mathbf{w}_3 \dots \mathbf{w}_m] [\tau_{12}^+ \quad \tau_3 \dots \tau_m]^T \end{cases} \quad (14)$$

The corresponding COWFW ( $f_{EE} = 500$  N,  $\eta = 1$ ) and COAWS are drawn in Fig. 6 and Fig. 7.

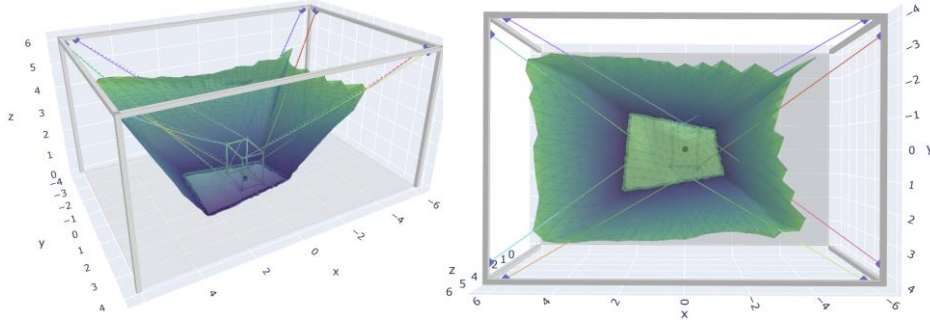


**Fig. 6.** COWFW of the example configuration where the translational EE is driven by a combination of cable 1 (blue) and cable 2 (red) against  $f_{EE}$  of 500 N with  $\eta = 1$ . Coordinates are in m.

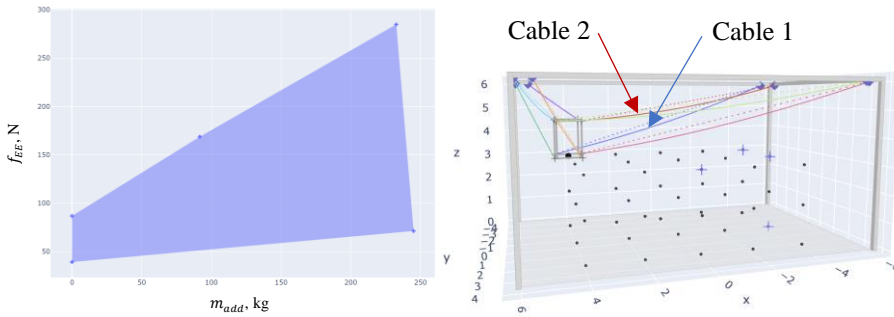


**Fig. 7.** COAWSs of the configuration with cable 1 and 2 driving antagonistically a translational EE DOF. Limiting positions are shown on the right as blue crosses. Black dots show non-limiting feasible positions which are part of the prescribed set of positions.

### 3.7 Discussion – Comparison of designs

A series of cable-driven configurations of an EE embedded in a CDPR mobile platform (internal EE), built from a CDPR configuration derived from the CoGiRo configuration detailed in Table 1, have been studied with respect to their workspace with a payload set at  $f_{EE} = 500$  N and payload capability within a designated workspace of 8 m x 5.3 m x 3 m. These results are compiled in Table 2.

**Table 2.** Example configuration drawing and fixing point coordinates in m.

EE drive	Sec tion	Workspace size with $f_{EE} = 500$ N (m)	Payload capabil- ity	Comments
Independent	3.3	9.6 x 6.3 x 4.0	261 kg	Effects of umbilical are neglected
One cable, di- rectly acting	3.4	(non-prismatic)	(217 to 261 kg)	Does not comply with the designated workspace
One doubled ca- ble, both acting antagonistically	3.5	Z = 0: 6.1 x 3.9 (off- set on XY) Z = 4: 9.6 x 6.2	261 kg, with $ f_{EE}  < 388$ N	Requires an additional winch with respect to original configuration
Two cables, act- ing antagonisti- cally	3.6	(non-prismatic – dra- matic effect at low Z)	245 kg, with $39 \text{ N} < f_{EE} < 284 \text{ N}$	Important impact on workspace; unidirectional $f_{EE}$ capacity

It is important to note that the capability in  $f_{EE}$  depends on the mass carried by the platform – with the possibility of using  $f_{EE}$  to carry such mass, and with possibility of integrating a speed reduction mechanism that amplifies force. The COAWS polygons as expressed in this paper, showing  $f_{EE}$  in function of added mass to the platform  $m_{add}$ , help determining the reduction ratio in function of the desired load.

Applying speed reduction impacts two parameters. The first parameter is EE velocity, since it will be reduced from the cable speed by the same ratio. The second parameter is, for the same reason, stroke. The stroke at the EE divided by the reduction ratio goes on top of the stroke required for the movement of the platform in the workspace in order to get the actual stroke required from the drum.

## 4 Conclusion and perspectives

The work presented in this paper is an initial approach to the topic. Many cable combinations being possible, using different sets of cables, with various reduction ratios and directions of pull, it is possible that other combinations than the ones presented here would deliver larger forces across the prescribed set of positions and/or have more limited impact on the static equilibrium and on workspace size. In order for the idea of using cables for driving EE to deliver high impact results, we will work in the future on a theoretical approach to evaluate the impact on the platform static equilibrium of any

combination of cables driving an EE. This will allow determining which of these combinations would lead to more favorable results. This theoretical approach should be generic so that it can be applied to any CDRP cable configuration and should exclude requiring additional winches. Besides, these developments are meant to lead towards the design of a  $m$ -cable CDRP with  $m$  degrees of freedom including internal translational and/or rotational EE DOFs.

## References

1. V. Nabat, M. Rodriguez, O. Company, S. Krut and F. Pierrot, "Par4: very high speed parallel robot for pick-and-place," in 2005 IEEE/RSJ International Conference on intelligent robots and systems, 2005.
2. S. Krut, O. Company, V. Nabat and F. Pierrot, "Heli4: a parallel robot for scara motions with a very compact traveling plate and a symmetrical design," in 2006 IEEE/RSJ International Conference on Intelligent Robots and Systems, 2006.
3. G. Wu, S. Bai and H. P., "Design analysis and dynamic modeling of a high-speed 3T1R pick-and-place parallel robot.," Recent Advances in Mechanism Design for Robotics - Mechanisms and Machine Science, vol. 33, pp. 285-295, 2015.
4. A. Fortin-Côté, C. Faure, L. Bouyer, B. J. McFadyen, C. Mercier, M. Bonenfant, D. Laurendeau, P. Cardou and C. Gosselin, "On the design of a novel cable-driven parallel robot capable of large rotation about one axis," Mechanisms and Machine Science, vol. 53, 2018.
5. C. Sun, H. Gao, Z. Liu, S. Xiang, H. Yu, N. Li and Z. Deng, "Design of spatial adaptive cable-driven parallel robots with an unlimited rotation axis using the cable wrapping phenomenon," Mechanism and Machine Theory, vol. 171, p. 104720, 2022.
6. L. Etienne, P. Cardou, M. Métillon and S. Caro, "Design of a planar cable-driven parallel crane without parasitic tilt," Journal of Mechanisms and Robotics, vol. 14, no. 4, p. 041006, 2022.
7. M. Métillon, P. Cardou, K. Subrin, C. Charron and S. Caro, "A cable-driven parallel robot with full-circle end-effector rotations," Journal of Mechanisms and Robotics, vol. 13, no. 3, 2021.
8. M. Métillon, "Novel Design for A Cable-Driven Parallel Robot with Full-Circle End-Effector Rotations," 09 08 2020. [Online]. Available: [https://youtu.be/JPYvRg7\\_Xbs](https://youtu.be/JPYvRg7_Xbs).
9. F. Gosselin, "Tight cable structure for e.g. haptic interface, has displacement unit displacing mobile member with respect to platform that is suspended inside framework by suspension cables, where unit is distinct to winders/unwinders of cables". France Patent FR2910833, 04 07 2008.
10. M. Gouttefarde, J. F. Collard, N. Riehl and C. Baradat, "Geometry selection of a redundantly actuated cable-suspended parallel robot," IEEE Transactions on Robotics, vol. 31, no. 2, pp. 501-510, 2015.
11. M. Gouttefarde, J.-F. Collard, N. Riehl and C. Baradat, "Simplified Analysis of Large-Dimension Parallel Cable-Driven Robots," in 2012 IEEE International Conference on Robotics and Automation, 2012.
12. S. Bouchard, C. Gosselin and B. Moore, "On the ability of a cable-driven robot to generate a prescribed set of wrenches," Journal of Mechanisms and Robotics, vol. 2, no. 1, p. 011010, 2010.